

Personalization Toolkit: Training Free Personalization of Large Vision Language Models

Soroush Seifi* Vaggelis Dorovatas* Matteo Cassinelli* Fabien Despinoy Daniel Olmeda
Reino Rahaf Aljundi

Toyota Motor Europe

Reviewed on OpenReview: <https://openreview.net/forum?id=5mbn3B0029>

Abstract

Personalization of Large Vision-Language Models (LVLMs) involves customizing models to recognize specific users or object instances and to generate contextually tailored responses. Existing approaches rely on time-consuming training for each item, making them impractical for real-world deployment, as reflected in current personalization benchmarks limited to object-centric single-concept evaluations. In this paper, we present a novel training-free approach to LVLM personalization called PeKit. We introduce a comprehensive, real-world benchmark designed to rigorously evaluate various aspects of the personalization task. PeKit leverages pre-trained vision foundation models to extract distinctive features, applies retrieval-augmented generation (RAG) techniques to identify instances within visual inputs, and employs visual prompting strategies to guide model outputs. Our model-agnostic vision toolkit enables efficient and flexible multi-concept personalization across both images and videos, without any additional training. We achieve state-of-the-art results, surpassing existing training-based methods.

1 Introduction

Large Vision Language Models (LVLMs) Liu et al. (2023a;b); Chen et al. (2024); Zhu et al. (2023); Li et al. (2023c); Agrawal et al. (2024); Wang et al. (2024) have demonstrated impressive capabilities in reasoning about visual content and answering visual questions across various domains. This suggests a great potential for deployment as visual assistants that can support users in their daily lives. However, current LVLMs are designed to provide generic, user-independent responses and recognize objects at the category level (Fig. 1, left).

The task of personalizing vision-language models was introduced by Alaluf et al. (2024) to enable LVLMs to recognize specific object instances and answer relevant questions accordingly. Existing approaches Alaluf et al. (2024); Nguyen et al. (2024) rely on training for a specific personalized object, diverting the LVLM from its original capabilities and incurring a large computational cost. Follow-up approaches attempted at replacing test-time training with large scale pretraining for the personalization task Pham et al. (2024); Pi et al. (2024), however, neither their effectiveness nor their scalability to various backbone models has been clearly demonstrated.

In this work, we argue that LVLM personalization can be approached without retraining the model parameters. We introduce a training-free approach that builds upon the strengths of pre-trained vision foundation models, the emerging capabilities of LLMs with in-context learning Dong et al. (2024) and retrieval-augmented generation (RAG) Lewis et al. (2020). Our method localizes instances using open-world object detectors Liu et al. (2023c); Kirillov et al. (2023); Oquab et al. (2023) and stores reference instance-level

*Providing contracted services at Toyota Motor Europe.

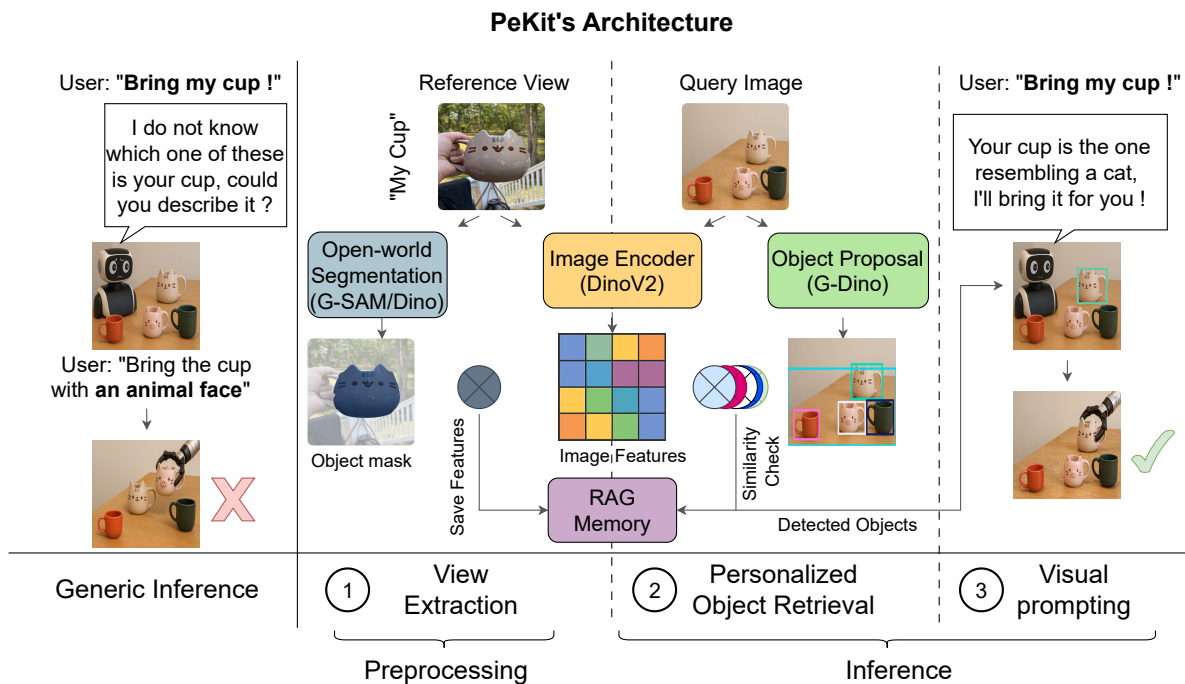


Figure 1: Illustration of the personalization task and PeKit. Left: Without personalization, VLMs often fail to resolve named object references, leading to ambiguous responses. Right: PeKit personalizes VLMs by (1) extracting patch-level features from a reference image into a RAG memory, (2) matching them with object proposals in the query image to retrieve the target object, and (3) guiding the VLM via visual prompting using the detected object’s bounding box and name. PeKit is VLM-agnostic, supports multi-concept personalization, handles video input, and achieves state-of-the-art (SOTA) performance, enabling capabilities often unsupported by prior methods.

features in memory banks, alongside their name and context. During inference, our retrieval module queries the memory bank and visual-prompts the LVLm. An overview of our approach is shown in Fig. 1.

With regards to the evaluation of personalization methodologies, existing benchmarks primarily focus on object-centric, single-concept tasks with the personalized instance prominently in the image, falling short of capturing the complexity of real-world applications where an AI assistant needs to understand multiple users and their belongings in dynamic scenes and environments. To address this gap, we introduce a novel and challenging benchmark derived from a video personalization dataset Yeh et al. (2023). Our benchmark not only features challenging single concept tasks but complex multi-concept interactions in addition to video question answering. We employ this benchmark to rigorously evaluate our method showing its effectiveness across diverse scenarios.

The key contributions of our work are: 1) We show that LVLm personalization is possible without training, enabling fast deployment. 2) We present a flexible method that supports multi-concept and video personalization across LVLms using vision foundation models, RAG, and visual prompting. 3) We introduce a challenging benchmark that exposes current limitations and guides future research.¹ 4) We achieve state-of-the-art performance on various tasks across both existing datasets and our proposed benchmark, consistently outperforming previous methods.

We discuss the related work in Section 2 followed by an introduction to our vision toolkit for LVLms personalization in Section 3. We then present our real-world benchmark and evaluate our approach in Section A.4, and conclude in Section 6.

¹Our benchmark and code will be available on Github.

2 Related Work

Text-to-Image Personalization. Personalizing text-to-image generation—i.e., generating images of a specific entity in novel contexts given a reference view—has been extensively explored. Early methods such as Textual Inversion Gal et al. (2022), DreamBooth Ruiz et al. (2023), and HyperDreamBooth Ruiz et al. (2024) achieve personalization by fine-tuning diffusion models for each entity, which limits scalability. More recent approaches, including InstantBooth Shi et al. (2024), JeDi Zeng et al. (2024), and Imagine He et al. (2024), circumvent this issue by pretraining for personalization, thereby eliminating the need for test-time fine-tuning.

Beyond generation, several works have explored personalized image retrieval using CLIP Radford et al. (2021) as the backbone. For example, PALAVRA Cohen et al. (2022) learns new concept tokens from a few user-provided images while keeping CLIP frozen, SEARLE Baldrati et al. (2023) maps reference images to pseudo-word tokens via a lightweight network and combines them with textual descriptions of desired changes for the Zero-Shot Composed Image Retrieval (ZS-CIR) task, and ConCon-Chi Rosasco et al. (2024) fuses image and text features through a learned composition network. In all these cases, retrieval is performed based on text-image similarity in CLIP space.

While these approaches focus on either text-to-image generation or retrieval, our work addresses a related but distinct challenge: identifying the same personalized object across different images and enabling personalized interactions with those objects through Large Vision-Language Models (LVLMs) such as LLaVA Liu et al. (2023b). We further posit that, unlike text-to-image personalization approaches that typically require training, personalization within LVLMs can be achieved without any adaptation of the underlying large language model.

Large Vision-Language Model Personalization. Personalizing LVLMs was first introduced in MyVLM Alaluf et al. (2024), which trains a concept head for specific objects on top of the CLIP CLS token. Similar to DreamBooth Ruiz et al. (2023), MyVLM uses rare tokens to encode personalized concepts, but this can introduce unintended behavior in language assistants and requires optimizing the LLM captioning loss for personalized conversations. Yo’LLaVA Nguyen et al. (2024) improves upon MyVLM by adding a dedicated token to the LLM head for each personalized object, learning concept tokens to describe them. However, this creates a challenging incremental classification problem De Lange et al. (2021), and like MyVLM, it requires test-time training for each new concept, limiting scalability to one concept at a time.

To avoid test-time training, recent works leverage large-scale pretraining. PVIT Pi et al. (2024) fine-tunes on synthetic personalized dialogues and uses reference images during inference. PLVLM Pham et al. (2024) aligns CLIP CLS and DINOv2 Oquab et al. (2023) embeddings with the LLM. Both works, primarily target individuals and do not support object-level personalization. Besides, personalization remains query-specific and is largely limited to VQA tasks.

In contrast, our approach introduces a modular, training-free framework that requires no retraining, scales naturally to multi-concept and video scenarios, and avoids relying on pre-trained tokens or reference images at inference time.

Finally, a concurrent work—Training-Free Personalization via Retrieval and Reasoning on Fingerprints Das et al. (2025)—also proposes a training-free framework. It derives textual and visual fingerprint attributes from reference images and employs multi-step reasoning to recognize personal concepts. While effective, this method depends on a complex, hand-engineered pipeline involving attribute extraction, chain-of-thought reasoning, cross-modal verification, and pairwise comparisons, making it vulnerable to hallucinated or noisy textual attributes generated by the underlying LVLM. By contrast, our approach uses a simpler patch-level matching strategy that avoids reliance on potentially hallucination-prone textual descriptions.

Visual Prompting. It represents the usage of visual cues such as bounding boxes or arrows to guide Vision-Language Models. CLIP Radford et al. (2021) interprets these marks to modify its CLS token embedding accordingly Shtedritski et al. (2023). Set of Mark Prompting Yang et al. (2023) integrates GPT-4V with visual prompts using tools like MaskDINO Li et al. (2023b), SAM Kirillov et al. (2023), Semantic SAM Li et al. (2023a), and SEEM Zou et al. (2024). ViPLLaVA Cai et al. (2024) enhances LLaVA Liu et al. (2023b)

to follow visual prompts by tuning on GPT-4V-labeled data. Contrastive Region Grounding (CRG) Wan et al. (2024) improves LLaVA’s focus on objects by contrasting token probabilities with and without target object masking. Our experiments show that LLaVA and other LVLMs can describe objects accurately with proper instruction and context. Training-free methods like CRG Wan et al. (2024) can further enhance attention if needed.

3 Approach

This section outlines our personalization toolkit, coined as *PeKit*, for enabling any LVLM to perform personalized detection and answer generation. We employ a three-stage pipeline: **View Extraction** to extract robust object-level features from reference images and store them in a memory module, **Personalized Objects Retrieval** to identify objects in the query image, and **Personalized Answer Generation** using visual prompting to generate user tailored and contextualized responses. We refer to Fig. 1 for an illustration of our approach.

3.1 Preliminary

We consider a given LVLM, a large language model with visual understanding capabilities and a set P of all personalized objects introduced to the LVLM. Each object $p \in P$ is associated with a set of reference images $\{I_p\}$, a name or identifier n_p and optionally c_p a context of the object. Our objective is to generate a personalized response for all images containing p during inference, while producing a general caption for any other image that does not contain any of the personalized objects. The LVLM, e.g., LLaVA Liu et al. (2023b) typically takes as input an input image I_p , a text query Q and additional text as context or instruction.

3.2 Training-free View Extraction

Existing LVLM personalization techniques depend on image-level representations of the objects’ training views Alaluf et al. (2024); Nguyen et al. (2024), which can lead to overfitting to the background of each object in the reference images, particularly for training-based approaches. To avoid such a bias, our method first localizes the object in the image and extracts only its corresponding features. We utilize an open-vocabulary segmentation network F_{ext} to extract object-level masks S_p based on each object’s generic category k_p which can be deduced from the name or the context²

$$S_p = F_{\text{ext}}(I_p, k_p). \tag{1}$$

We construct the average embedding vector \mathbf{e}_p for object p by average pooling of the embedding vectors produced by the image encoder F_{emb} on the image I_p over the region defined by the object-level mask S_p :

$$\mathbf{e}_p = \text{AvgPool}(F_{\text{emb}}(I_p), S_p) \in \mathbb{R}^{D_h}. \tag{2}$$

Considering N reference images, we concatenate all object embedding vectors \mathbf{e}_p^i (of the object p pooled over the i -th reference image I_p^i) into a matrix $E_p = [\mathbf{e}_p^1, \dots, \mathbf{e}_p^N] \in \mathbb{R}^{D_h \times N}$.

Memory module. After extracting the personalized objects’ embeddings, we store each object’s relevant properties in our memory module. The memory module is represented by a set \mathcal{M} of object-specific entries:

$$\mathcal{M} = \{(E_p, (n_p, c_p))\}_{p \in P}, \tag{3}$$

where n_p is the identifier or the name of the personalized object p , and c_p is the context of the object, which can contain prior knowledge such as characteristics, background story or even relation to other personalized objects. When the number of personalized objects scales, the memory module \mathcal{M} is easily converted into a Vector database, where nearest neighbor approximate search is deployed to retrieve instances matching a given query Han et al. (2023) ensuring efficiency and scalability.

²Although using the semantic category k_p is recommended for optimal performance, our method attains state-of-the-art results even without it, relying solely on the generic category ‘main’. See section 4.7.1 for further discussion.

3.3 Personalized Object Retrieval

During inference, our goal is to determine whether a personalized object is present in the provided image I . We use any available object proposal technique F_{prop} to generate a set of proposals (e.g., bounding boxes) $O = \{o_i\} = F_{\text{prop}}(I)$ for potential object occurrences within the image I . Then for each proposal o_i , we calculate its object-level average embedding vector:

$$\mathbf{e}_{o_i} = \text{AvgPool}(F_{\text{emb}}(I), o_i). \quad (4)$$

We define the retrieval module \mathcal{R} that takes an object embedding vector \mathbf{e}_{o_i} and retrieves the memory entry $(E_j, (n_j, c_j))$ for a matching object j as:

$$\mathcal{R}(\mathbf{e}_{o_i}) = \begin{cases} (E_j, (n_j, c_j)), & \text{if } j = \arg \max_l \{\text{sim}(E_l, \mathbf{e}_{o_i})\} \\ & \text{and } \text{sim}(E_j, \mathbf{e}_{o_i}) > \tau \\ \phi, & \text{otherwise} \end{cases} \quad (5)$$

where $\text{sim}(E_l, \mathbf{e}_{o_i}) = \arg \max_k \{\text{sim}(\mathbf{e}_l^k, \mathbf{e}_{o_i})\}$. We calculate the proposal’s similarity to the embeddings of the training views for all personalized objects. Any similarity measure (e.g., cosine similarity) can be employed for this purpose. We set a constant threshold τ to identify the personalized objects. We discard the object proposals in which no matching object is found by the retrieval module \mathcal{R} . Our method inherently supports the detection of multiple personalized objects.

3.4 Personalized Answer Generation

Once a personalized object is identified, our method generates captions specifically about that object, distinct from general captions a standard LVLM would produce. This involves emphasizing the detected object and incorporating prior knowledge about it. We achieve this through visual prompting by overlaying bounding boxes on the image and querying the LVLM to generate captions or answer questions focused on these objects. We use distinctive colors to differentiate recognized objects. We provide the LVLM with the object identifier n_j (e.g., the instance name) and possibly a context c_j for each personalized object. The LVLM incorporates this context and responds to queries using the given name n_j . For multiple personalized objects, we instruct the LVLM for each bounding box, name, and context. We refer to Appendix C.1 for the exact prompt format.

3.5 Video-personalization

To conduct personalized video question answering (VQA), we apply our method to the video frames. We first identify any presence of a personalized object, then each personalized object is consistently visually prompted using the same bounding box color across all frames to maintain identity. The video frames—including those with visual prompts and those without any detected personalized objects—are fed into a video large language model.

The model is then prompted to generate captions or answer questions using each detected object’s identifier n_j , an optional context c_j , and the unique bounding box color used for the visual prompting of that object instance (Appendix C.1).

3.6 Choice of Vision Tools

We deploy GroundedSAM Ren et al. (2024) as the segmentation network F_{ext} and ablate using GroundingDINO Liu et al. (2023c), where the mask is represented by the object’s bounding box. We use DINOv2 Oquab et al. (2023) as the image encoder F_{emb} to extract patch-level features of the objects and ablate using CLIP Radford et al. (2021) in Appendix A.1. During inference, GroundingDINO Liu et al. (2023c) is queried with the term ‘object’ to generate object proposals.



Figure 2: Our proposed evaluation set *This-Is-My-Img*, built on the *This-Is-My* dataset Yeh et al. (2023): Example reference views and validation samples from the single-concept category ‘Reynard’s Work Chair’ and the multi-concept category ‘Nikki’ and ‘Nikki’s Car’.

4 Experiments

In this section we present the considered benchmarks and introduce our LVLm personalization benchmark. We then compare our approach with SOTA personalization methods and baselines under various settings.

4.1 Existing Benchmarks

We consider the datasets from **Yo’LLaVA** Nguyen et al. (2024) and **MyVLM** Alaluf et al. (2024). Yo’LLaVA includes 40 categories of objects, buildings, and people, with 4–10 images per category for training and validation. It also features a VQA benchmark with multiple-choice questions (A/B). MyVLM comprises 29 object categories, each with 7–17 images, using 4 images for training and the rest for validation, with final accuracies averaged over 5 runs. For both datasets, we use only reference images and the semantic category of each object for training view extraction (see 3.2), discarding all other data, such as the ground-truth captions and negative images.

4.2 Real-world Personalization Benchmark

Yo’LLaVA Nguyen et al. (2024) and **MyVLM** Alaluf et al. (2024) focus mainly on object-centric scenes under controlled conditions, lacking real-world complexity such as background clutter, occlusion, and diverse contexts—limiting their suitability for evaluating robust LVLm personalization.

We introduce the **This-Is-My-Img** benchmark, derived from the *This-Is-My* dataset Yeh et al. (2023), originally designed for video-level detection of personalized objects in realistic environments. Our benchmark includes several splits targeting specific personalization capabilities.

Reference Views: Five reference frames per object extracted from training segments. Unlike prior datasets, objects here may be partially visible, distant, or poorly lit (see Fig. 5, Appendix).

Single-Concept Eval Set: Set of images designed to evaluate a single personalized object. Fig. 2 shows examples. For each personalized object, images are labeled as:

- *Positive*: Includes only images where the personalized object appears and is used to test how well the method can correctly detect all occurrences of that object, that is, recall or *positive accuracy* in Yo’LLaVA Nguyen et al. (2024) and MyVLM Alaluf et al. (2024).

- *Negative (Hard)*: Images taken from video segments of the personalized object **where the object is not visible**. This tests method’s overfitting to the background associated with the personalized object in the reference views.
- *Negative (Other)*: Images sourced from video segments of other personalized objects. This set measures method’s robustness to intra-instance and the general dataset bias.
- *Negative (Fake)*: AI-generated images (via GPT-4o) that mimic the personalized object in different perspectives and environments while making sure the specific characteristics of the fake object are different from the real personalized object. These samples are used to assess the robustness of the methods against high visual similarity combined with a distribution shift.
- *Single-Concept VQA*: Multiple choice questions based on positive images, following the Yo’LLaVA benchmark VQA format.

Multi-Concept Set: This subset comprises images containing pairs of personalized concepts, such as person–object pairs or person–person pairs, fig 2. We extend the personalized instances from the original This-Is-My dataset with additional instances that frequently co-occur with them. For each pair, we collect all images containing both personalized concepts and partition them into two subsets. Positive samples include images in which both concepts appear simultaneously, whereas negative samples comprise images from all other pairs. Illustrative examples are presented in Fig. 2.

- *Multi-Concept VQA*: This component provides open-ended questions associated with each image in the multi-concept set, addressing both personalized concepts depicted. The set includes 55 images and their corresponding QA pairs.

Video-QA Set: Original video clips from This-Is-My dataset are coupled with open-ended questions regarding the personalized object in each video, designed to evaluate both temporal reasoning and the method adaptability to video-based inputs.

Overall, This-Is-My-Img offers a comprehensive and realistic benchmark for LVLm personalization, requiring accurate recognition and reasoning over personalized objects in cluttered and dynamic conditions. See Appendix B for more details on our proposed benchmark.

4.3 Metrics and Evaluation Setting

Single-Concept Metrics. We adopt the metrics and notation from Yo’LLaVA Nguyen et al. (2024) and MyVLM Alaluf et al. (2024). We report *Positive Accuracy (Recall)*—the proportion of correctly identified positives, *Negative Accuracy (Specificity)*—correctly identified negatives, and *Weighted Accuracy*, their average across n personalized objects. We also include *Precision*, the ratio of true to predicted positives, averaged over n objects, to capture the accuracy–precision trade-off. For single-concept VQA, accuracy is the percentage of correctly answered multiple-choice questions. Following MyVLM, we additionally report *CLIPScore* (caption–image similarity) and *Personalization Recall*, the fraction of captions correctly mentioning the target concept.

Multi-Concept Metrics. Positive accuracy measures images where both personalized objects are correctly detected; negative accuracy covers those where at least one is correctly **not** detected.

Video and Multi-Concept VQA Metric. For open-ended VQA, we use an autograding protocol Maaz et al. (2023) with ChatGPT-3.5 to assess contextual similarity between predicted and ground-truth answers (see Appendix C.2).

Implementation Details. The modularity of our method makes it generic regarding the choice of the LVLm model. We use LLaVA1.5-13B Liu et al. (2023a) as our primary LVLm model for consistency with previous works. We pair PeKit with InternVL2-26B Chen et al. (2024), a state-of-the-art LVLm to ablate. We use LLaVA-OneVision-Qwen2-7B as our default video model and ablate with InternVideoChat2.5 as a superior video model. We utilize Cosine Similarity with a constant threshold of $\tau=0.75$ for detecting

Table 1: Visual recognition performance (%) on existing datasets. PeKit achieves state of the art performance without training. Cited entries are taken from their respective papers.

MyVLM Dataset				
Method/Metric	Precision	Accuracy		
		Positive	Negative	Weighted
MyVLM Alaluf et al. (2024)	–	96.6	90.9	93.8
Yo’LLaVA Nguyen et al. (2024)	–	97.0	95.7	96.4
PeKit (G-DINO)	<u>79.1</u>	94.3	<u>98.8</u>	96.5
PeKit (G-SAM)	82.3	97.6	99.0	98.3
Yo’ LLaVA Dataset				
Method/Metric	Precision	Accuracy		
		Positive	Negative	Weighted
Yo’LLaVA Nguyen et al. (2024)	–	94.9	89.8	92.4
PeKit (G-DINO)	77	89.9	98.9	<u>94.4</u>
PeKit (G-SAM)	<u>74.8</u>	<u>91.0</u>	<u>98.7</u>	94.9

Table 2: Visual recognition accuracy (%) on the This-Is-My-Img dataset. MyVLM and Yo’LLaVA produce many false positives in a challenging real-world scenario.

(a) Single-concept results.

Method/Metric	Precision	Accuracy				Avg.
		Pos.	Other	Hard	Fake	
MyVLM	8.0	88.1	14.6	4.7	54.2	33.9
Yo’LLaVA	42.1	87.1	84.4	61.9	61.4	67.3
Ours	90.1	69.0	99.9	96.0	59.3	82.8

(b) Multi-concept results.

Method/Metric	Precision	Accuracy		Avg.
		Pos.	Neg.	
Yo’LLaVA	10.0	83.6	25.0	54.3
Ours	96.1	45.4	99.8	72.6

personalized objects across all datasets (3.3). Refer to Appendix A.6 for further details on compute and memory overhead of our personalization toolkit.

4.4 Visual-Recognition

Previous Datasets Tab. 1 compares our method to MyVLM Alaluf et al. (2024) and Yo’LLaVA Nguyen et al. (2024) on their respective benchmarks. On MyVLM benchmark, PeKit achieves a new SOTA, improving both positive and negative accuracy with an average gain of 1.9%. On Yo’LLaVA benchmark, it increases negative accuracy by 8.9%, with slightly lower positive accuracy, resulting in a 2.5% improvement in weighted accuracy. While PeKit may miss some difficult instances, its low false positive rate helps avoid incorrect personalized outputs, favoring generic captions when uncertain. We ablate the choice of an open-world object detector, G-DINO Liu et al. (2023c), compared to the open-world semantic segmentation model, G-SAM Ren et al. (2024), for F_{ext} in Eq. 1. The results show that our method outperforms previous methods in both cases. However, the more precise segmentation model, which extracts only patches of the object of interest, achieves the best accuracy on average.

Table 3: Captioning metrics on MyVLM dataset. Higher is better.

Method	CLIPScore	Personal. Recall
MyVLM Alaluf et al. (2024)	<u>27.6</u>	<u>94.76</u>
PeKit (LLaVA)	30.2	97.1

Table 4: Single-concept VQA accuracy on Yo’LLaVA and This-Is-My-Img datasets.

Yo’LLaVA VQA Accuracy		This-Is-My-Img Single-Concept VQA Accuracy	
LLaVA Nguyen et al. (2024)	89.9	LLaVA	72.8
Yo’LLaVA Nguyen et al. (2024)	92.9	Yo’LLaVA	67.1
PeKit (LLaVA)	<u>93.4</u>	PeKit (LLaVA)	<u>77.1</u>
PeKit (InternVL)	95.9	PeKit (InternVL)	84.2

This-Is-My-Img Benchmark. Tab. 2 summarizes benchmark performance. For single-concept images, **MyVLM** achieves high positive accuracy but poor negative accuracy (14.6% on *other*, 4.7% on *hard*), indicating a bias toward positive responses and reliance on scene context over object details. **Yo’LLaVA** performs similarly but better (87.1% positive, 84.8% on *other*, 61.9% on *hard*). In contrast, **PeKit** attains much stronger negative accuracy (99.9%, 96.0%) and 90.1% precision—48% higher than Yo’LLaVA—showing far fewer false positives.

On fake images, differences narrow. All models struggle with stylistically similar objects; image-level approaches like MyVLM and Yo’LLaVA slightly better detect domain shifts. Nonetheless, PeKit remains robust to domain variation despite some difficulty with near-identical objects, achieving the best overall balance with 82.86% average accuracy, surpassing Yo’LLaVA (67.38%) and MyVLM (33.92%).

In multi-concept settings, PeKit shows slightly lower dual-object accuracy but far higher precision and negative accuracy, yielding an 18.3% overall gain over Yo’LLaVA. These results highlight our training-free method’s robustness and low false-positive rate, especially in complex, real-world scenarios.

Overall, this evaluation underscores the challenge of personalization beyond object-centric imagery, advancing toward realistic benchmarks for intelligent visual assistants.

4.5 Visual-Question Answering

Tabs. 3, 4, and 5 evaluate PeKit on personalized object VQA across multiple scenarios using the Yo’LLaVA Nguyen et al. (2024) and This-Is-My-Img benchmarks. For completeness, we also compare against MyVLM on its dataset using CLIPScore Hessel et al. (2021) and Personalization Recall, as it lacks a VQA split.

PeKit consistently outperforms baselines on both single- and multi-concept VQA tasks. On the MyVLM dataset, PeKit surpasses MyVLM in generating image-aligned captions (CLIPScore) and correctly referencing personalized concepts (Personalization Recall). On the Yo’LLaVA benchmark, PeKit outperforms Yo’LLaVA without requiring any fine-tuning, special tokens, or model modifications.

On the This-Is-My-Img benchmark, Yo’LLaVA performs on par with the base LLaVA, while PeKit yields a 5% improvement, showing strong visual recognition and reasoning. In multi-concept cases, Yo’LLaVA degrades base model performance, whereas PeKit delivers a consistent 7% gain. Moreover, PeKit generalizes effectively to the video domain (3.5), unlike prior approaches, which are not readily extendable to video. PeKit improves the base model by 12% and maintains gains when combined with stronger instruction-following backbones.

In summary, our experiments demonstrate that PeKit consistently outperforms training-based personalization methods across diverse benchmarks, including single- and multi-concept VQA tasks. Its ability to

Table 5: VQA accuracy on **This-Is-My-Img Multi-Concept** and **This-Is-My-Video** datasets.

This-Is-My-Img Multi-Concept VQA Accuracy		This-Is-My-Video VQA Accuracy	
LLaVA	49.0	LLaVA-OneVision-Qwen2	23.0
Yo’LLaVA	12.7	PeKit (LLaVA-OneVision-Qwen2)	35.0
PeKit (LLaVA)	<u>56.3</u>	InternVideoChat2.5	<u>56.6</u>
PeKit (InternVL)	63.6	PeKit (InternVideoChat2.5)	61.3

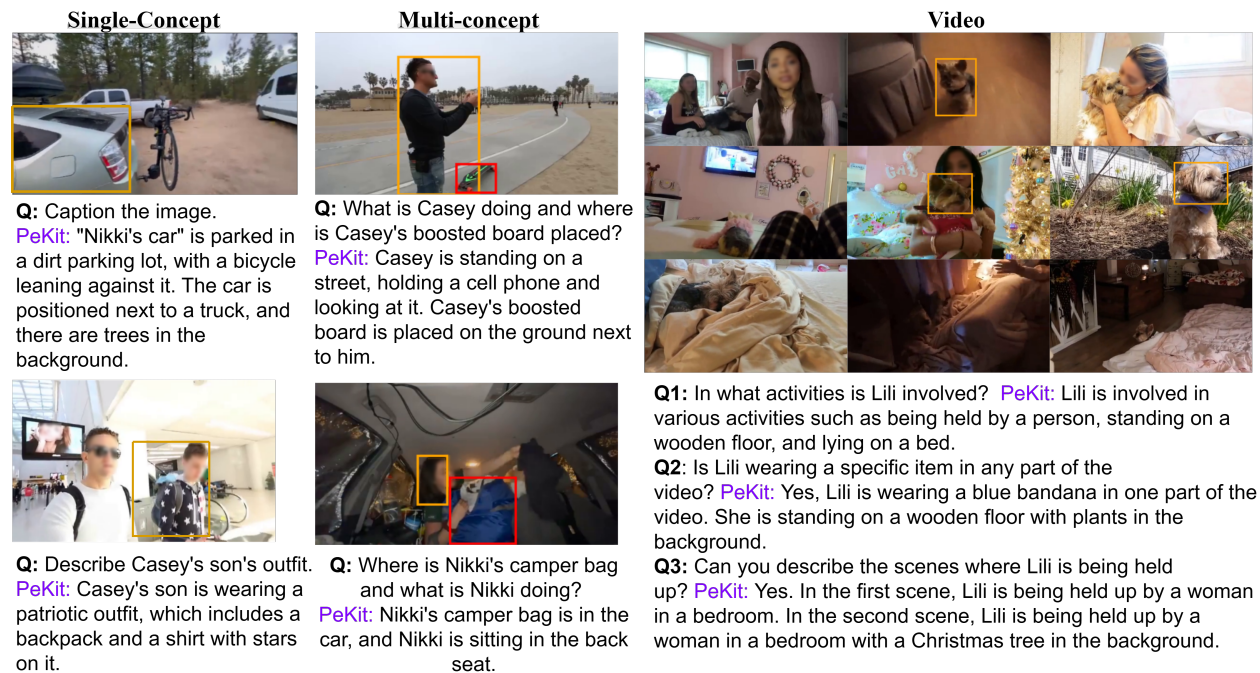


Figure 3: **Qualitative Results:** PeKit handles a range of personalization tasks, encompassing both single- and multi-concept personalization in images and videos. For video personalization, the VLM model can reliably track the target object across frames using only a few confidently annotated instances. One representative frame is shown per scene.

generalize without fine-tuning, maintain performance in multi-concept scenarios, and extend effectively to video settings highlights its robustness and scalability for real-world personalized visual understanding.

4.6 Qualitative Results

Fig. 3 presents examples of PeKit performing various tasks on the proposed benchmark, This-Is-My-Img. In the left column, PeKit successfully identifies personalized single-concept objects, even in ambiguous scenarios involving multiple instances from the same object category. In the middle column, it demonstrates the ability to answer questions involving multi-concept pairs. Lastly, without any modifications, the model can be applied to video inputs by visually prompting the model with detected personalized objects in the video. Further qualitative comparisons with the base LLaVA model, MyVLM, and Yo’LLaVA are presented in Appendices D.1, D.2, and D.3.

4.7 Ablation and Analysis

A comprehensive analysis of our method is provided in Appendix.A, where we analyze robustness under various settings. Specifically, we examine the effects of altering the backbone encoder F_{emb} , the number

of reference images per object (N), the number of personalized objects (P) in the dataset, the detection threshold (τ) and the name (n_p) of the personalized objects.

In the following subsection, we additionally examine the robustness of our approach with respect to a requirement introduced by our framework, namely the semantic category k_p assigned to each object (see Section 3.2).

4.7.1 Semantic Category k_p

As described in Section 3.2, we use the semantic category k_p of each object in the reference image I_p to derive its corresponding object-level mask S_p .

We note that, in practice, introducing an object for personalization typically involves specifying its name. In many cases, the name itself implicitly encodes the semantic category—e.g., ‘My book’ or ‘Jack’s car’—which can then be leveraged by an open-vocabulary segmentation model for view extraction.

Therefore, for the MyVLM dataset, where the object names are generic, we directly input them into our open-vocabulary detector. Similarly, on This-Is-My-Img dataset, aside from the people in the dataset (queried with the category ‘Man/Woman’), all other object names in this dataset include their semantic category (e.g., Alex’s hat, See Appendix.B).

For the Yo’LLaVA dataset, some concept names such as Vietnamese individual names do not directly indicate the semantic categories. We compare our method’s performance on the Yo’LLaVA dataset by providing the open-vocabulary segmentation model with semantic categories, dataset-provided names, or the generic term ‘main’ during reference view extraction. As shown in Table 6, PeKit achieves state-of-the-art performance even without relying on semantic categories of personalized objects. Note that during inference we consistently use the term ‘object’ to extract object proposals using G-Dino.

Consequently, when the reference image for a personalized object is representative, with the subject clearly dominating the scene, our method remains competitive even without an explicitly provided semantic category k_p . If needed, a lightweight open-world classifier can be employed to infer this label prior to processing the object within our pipeline.

Table 6: Reference view vocabulary ablation on Yo’LLaVA dataset. PeKit achieves SOTA results even using the generic category ‘main’ to extract the personalized objects from the reference views.

Method/Metric	Precision	Positive Acc	Negative Acc	Weighted Acc
Yo’ LLaVA	-	94.9	89.8	92.4
PeKit (categories)	74.8	<u>91</u>	<u>98.7</u>	94.9
PeKit (‘main’)	72.9	86.9	98.9	92.9
PeKit (Vietnamese names)	<u>73.8</u>	88	98.9	<u>93.45</u>

5 Limitations and Future Work

5.1 Noisy Reference Views

Our method relies on instance masks generated by a segmentation network. Inaccurate or noisy masks can lead to false positives during inference. As shown in Figure 4, poor masks (highlighted in red) result in incorrect matches (red bounding boxes). Applying clustering to reference features may help filter out erroneous views and improve matching reliability.

5.2 Small Object Representation

Due to the stride factor (=14) in the DINOv2 encoder, feature extraction occurs at a lower resolution than the original image. This limits detail capture for small objects, as illustrated in Figure 5, where only coarse features (e.g., color or category) are encoded, increasing false positives. A potential solution is to crop and resize small objects to DINOv2’s native resolution (518×518) before embedding.

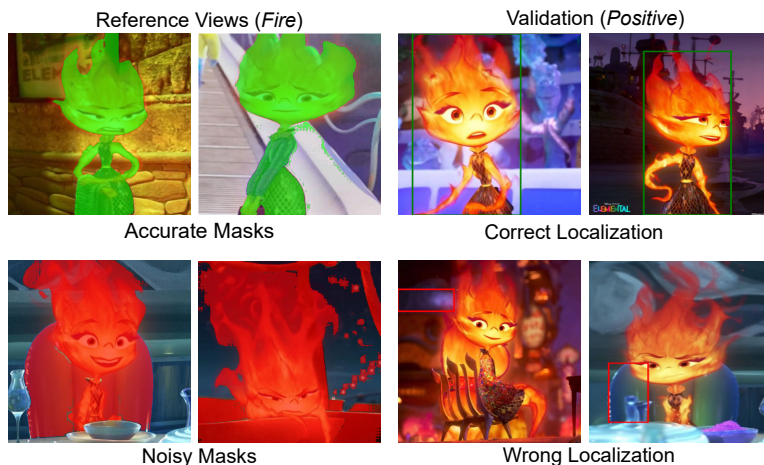


Figure 4: Noisy reference views: Poor segmentation masks may affect the visual prompting stage and degrade PeKit’s performance.



Figure 5: Small reference objects: Due to DINO’s fixed patch size of 14×14 , the resulting embeddings are relatively coarse, which can lead to increased false positives, especially for small or fine-grained objects.

5.3 Contextual Object Relationships

Our instance-level detection approach could benefit from contextual cues. For example, identifying *Alex’s everyday bag* is more reliable when *Alex* is present in the scene. Future work will explore extracting object relationships from reference images and integrating them into the LVLM as prior knowledge.

6 Discussion and Conclusion

In this work, we introduced PeKit, a training-free, plug-and-play toolkit for LVLM personalization that combines vision foundation models with retrieval-augmented generation and visual prompting. Our approach outperforms existing training-based methods without requiring any fine-tuning or additional data beyond the personalized concept inputs. To evaluate our method, we proposed a challenging new benchmark that reflects more realistic scenarios involving multi-concept and video personalization, significantly increasing the complexity of the visual recognition task. PeKit demonstrates strong robustness and scalability across both multi-concept and video settings. Our benchmark reveals strong performance and shows some improvement points, particularly in handling complex temporal and multi-concept reasoning. We believe that PeKit establishes a new efficient training-free baseline for future research in LVLM personalization.

7 Ethical Considerations

PeKit is a training-free personalization approach for LVLMs designed to assist users in everyday tasks. It enables local and efficient customization without the need for retraining, supporting applications such as personalized robotics and visual assistants (see Figure 1 and Figure 10 Appendix).

We recognize potential risks if the method were misused for surveillance or applied without user consent. To address these concerns, PeKit operates entirely on-device, never transmits data externally, and works on extracted features rather than storing raw images. Personalization remains fully user-controlled, requiring explicit input.

References

- Pravesh Agrawal, Szymon Antoniak, Emma Bou Hanna, Baptiste Bout, Devendra Chaplot, Jessica Chudnovsky, Diogo Costa, Baudouin De Monicault, Saurabh Garg, Theophile Gervet, Soham Ghosh, Amélie Héliou, Paul Jacob, Albert Q. Jiang, Kartik Khandelwal, Timothée Lacroix, Guillaume Lample, Diego Las Casas, Thibaut Lavril, Teven Le Scao, Andy Lo, William Marshall, Louis Martin, Arthur Mensch, Pavankumar Muddireddy, Valera Nemychnikova, Marie Pellat, Patrick Von Platen, Nikhil Raghuraman, Baptiste Rozière, Alexandre Sablayrolles, Lucile Saulnier, Romain Sauvestre, Wendy Shang, Roman Soletskyi, Lawrence Stewart, Pierre Stock, Joachim Studnia, Sandeep Subramanian, Sagar Vaze, Thomas Wang, and Sophia Yang. Pixtral 12b, 2024. URL <https://arxiv.org/abs/2410.07073>.
- Yuval Alaluf, Elad Richardson, Sergey Tulyakov, Kfir Aberman, and Daniel Cohen-Or. Myvlm: Personalizing vlms for user-specific queries. *arXiv preprint arXiv:2403.14599*, 2024.
- Alberto Baldrati, Lorenzo Agnolucci, Marco Bertini, and Alberto Del Bimbo. Zero-shot composed image retrieval with textual inversion. In *Proceedings of the IEEE/CVF International Conference on Computer Vision*, pp. 15338–15347, 2023.
- Mu Cai, Haotian Liu, Siva Karthik Mustikovela, Gregory P Meyer, Yuning Chai, Dennis Park, and Yong Jae Lee. Vip-llava: Making large multimodal models understand arbitrary visual prompts. In *Proceedings of the IEEE/CVF Conference on Computer Vision and Pattern Recognition*, pp. 12914–12923, 2024.
- Zhe Chen, Jiannan Wu, Wenhai Wang, Weijie Su, Guo Chen, Sen Xing, Muyan Zhong, Qinglong Zhang, Xizhou Zhu, Lewei Lu, et al. Internvl: Scaling up vision foundation models and aligning for generic visual-linguistic tasks. In *Proceedings of the IEEE/CVF Conference on Computer Vision and Pattern Recognition*, pp. 24185–24198, 2024.
- Tianheng Cheng, Lin Song, Yixiao Ge, Wenyu Liu, Xinggang Wang, and Ying Shan. Yolo-world: Real-time open-vocabulary object detection. In *Proc. IEEE Conf. Computer Vision and Pattern Recognition (CVPR)*, 2024.
- Niv Cohen, Rinon Gal, Eli A Meir, Gal Chechik, and Yuval Atzmon. “this is my unicorn, fluffy”: Personalizing frozen vision-language representations. In *European conference on computer vision*, pp. 558–577. Springer, 2022.
- Deepayan Das, Davide Talon, Yiming Wang, Massimiliano Mancini, and Elisa Ricci. Training-free personalization via retrieval and reasoning on fingerprints. *arXiv preprint arXiv:2503.18623*, 2025.
- Matthias De Lange, Rahaf Aljundi, Marc Masana, Sarah Parisot, Xu Jia, Aleš Leonardis, Gregory Slabaugh, and Tinne Tuytelaars. A continual learning survey: Defying forgetting in classification tasks. *IEEE transactions on pattern analysis and machine intelligence*, 44(7):3366–3385, 2021.
- Yinan Deng, Bicheng Yao, Yihang Tang, Yi Yang, and Yufeng Yue. Openvox: Real-time instance-level open-vocabulary probabilistic voxel representation. *arXiv preprint arXiv:2502.16528*, 2025.
- Qingxiu Dong, Lei Li, Damai Dai, Ce Zheng, Jingyuan Ma, Rui Li, Heming Xia, Jingjing Xu, Zhiyong Wu, Baobao Chang, et al. A survey on in-context learning. In *Proceedings of the 2024 Conference on Empirical Methods in Natural Language Processing*, pp. 1107–1128, 2024.

- Rinon Gal, Yuval Alaluf, Yuval Atzmon, Or Patashnik, Amit H Bermano, Gal Chechik, and Daniel Cohen-Or. An image is worth one word: Personalizing text-to-image generation using textual inversion. *arXiv preprint arXiv:2208.01618*, 2022.
- Yikun Han, Chunjiang Liu, and Pengfei Wang. A comprehensive survey on vector database: Storage and retrieval technique, challenge. *arXiv preprint arXiv:2310.11703*, 2023.
- Zecheng He, Bo Sun, Felix Juefei-Xu, Haoyu Ma, Ankit Ramchandani, Vincent Cheung, Siddharth Shah, Anmol Kalia, Harihar Subramanyam, Alireza Zareian, et al. Imagine yourself: Tuning-free personalized image generation. *arXiv preprint arXiv:2409.13346*, 2024.
- Jack Hessel, Ari Holtzman, Maxwell Forbes, Ronan Le Bras, and Yejin Choi. Clipscore: A reference-free evaluation metric for image captioning. *arXiv preprint arXiv:2104.08718*, 2021.
- Alexander Kirillov, Eric Mintun, Nikhila Ravi, Hanzi Mao, Chloe Rolland, Laura Gustafson, Tete Xiao, Spencer Whitehead, Alexander C Berg, Wan-Yen Lo, et al. Segment anything. In *Proceedings of the IEEE/CVF International Conference on Computer Vision*, pp. 4015–4026, 2023.
- Patrick Lewis, Ethan Perez, Aleksandra Piktus, Fabio Petroni, Vladimir Karpukhin, Naman Goyal, Heinrich Küttler, Mike Lewis, Wen-tau Yih, Tim Rocktäschel, et al. Retrieval-augmented generation for knowledge-intensive nlp tasks. *Advances in Neural Information Processing Systems*, 33:9459–9474, 2020.
- Feng Li, Hao Zhang, Peize Sun, Xueyan Zou, Shilong Liu, Jianwei Yang, Chunyuan Li, Lei Zhang, and Jianfeng Gao. Semantic-sam: Segment and recognize anything at any granularity. *arXiv preprint arXiv:2307.04767*, 2023a.
- Feng Li, Hao Zhang, Huaizhe Xu, Shilong Liu, Lei Zhang, Lionel M Ni, and Heung-Yeung Shum. Mask dino: Towards a unified transformer-based framework for object detection and segmentation. In *Proceedings of the IEEE/CVF Conference on Computer Vision and Pattern Recognition*, pp. 3041–3050, 2023b.
- Junnan Li, Dongxu Li, Silvio Savarese, and Steven Hoi. Blip-2: Bootstrapping language-image pre-training with frozen image encoders and large language models. In *International conference on machine learning*, pp. 19730–19742. PMLR, 2023c.
- Haotian Liu, Chunyuan Li, Yuheng Li, and Yong Jae Lee. Improved baselines with visual instruction tuning. In *Proceedings of the IEEE/CVF Conference on Computer Vision and Pattern Recognition*, pp. 26296–26306, 2023a.
- Haotian Liu, Chunyuan Li, Qingyang Wu, and Yong Jae Lee. Visual instruction tuning. *Advances in neural information processing systems*, 36, 2023b.
- Shilong Liu, Zhaoyang Zeng, Tianhe Ren, Feng Li, Hao Zhang, Jie Yang, Qing Jiang, Chunyuan Li, Jianwei Yang, Hang Su, et al. Grounding dino: Marrying dino with grounded pre-training for open-set object detection. *arXiv preprint arXiv:2303.05499*, 2023c.
- Muhammad Maaz, Hanoona Rasheed, Salman Khan, and Fahad Shahbaz Khan. Video-chatgpt: Towards detailed video understanding via large vision and language models. *arXiv preprint arXiv:2306.05424*, 2023.
- Mohammad Mohammadi, Daniel Honerkamp, Martin Büchner, Matteo Cassinelli, Tim Welschhold, Fabien Despinoy, Igor Gilitschenski, and Abhinav Valada. More: Mobile manipulation rearrangement through grounded language reasoning. *IEEE/RSJ International Conference on Intelligent Robots and Systems (IROS)*, 2025.
- Thao Nguyen, Haotian Liu, Yuheng Li, Mu Cai, Utkarsh Ojha, and Yong Jae Lee. Yo’llava: Your personalized language and vision assistant. *arXiv preprint arXiv:2406.09400*, 2024.
- Maxime Oquab, Timothée Darcet, Théo Moutakanni, Huy Vo, Marc Szafraniec, Vasil Khalidov, Pierre Fernandez, Daniel Haziza, Francisco Massa, Alaaeldin El-Nouby, et al. Dinov2: Learning robust visual features without supervision. *arXiv preprint arXiv:2304.07193*, 2023.

- Chau Pham, Hoang Phan, David Doermann, and Yunjie Tian. Personalized large vision-language models, 2024. URL <https://arxiv.org/abs/2412.17610>.
- Renjie Pi, Jianshu Zhang, Tianyang Han, Jipeng Zhang, Rui Pan, and Tong Zhang. Personalized visual instruction tuning. *arXiv preprint arXiv:2410.07113*, 2024.
- Alec Radford, Jong Wook Kim, Chris Hallacy, Aditya Ramesh, Gabriel Goh, Sandhini Agarwal, Girish Sastry, Amanda Askell, Pamela Mishkin, Jack Clark, et al. Learning transferable visual models from natural language supervision. In *International conference on machine learning*, pp. 8748–8763. PMLR, 2021.
- Tianhe Ren, Shilong Liu, Ailing Zeng, Jing Lin, Kunchang Li, He Cao, Jiayu Chen, Xinyu Huang, Yukang Chen, Feng Yan, et al. Grounded sam: Assembling open-world models for diverse visual tasks. *arXiv preprint arXiv:2401.14159*, 2024.
- Andrea Rosasco, Stefano Berti, Giulia Pasquale, Damiano Malafra, Shogo Sato, Hiroyuki Segawa, Tetsugo Inada, and Lorenzo Natale. Concon-chi: Concept-context chimera benchmark for personalized vision-language tasks. In *Proceedings of the IEEE/CVF Conference on Computer Vision and Pattern Recognition*, pp. 22239–22248, 2024.
- Nataniel Ruiz, Yuanzhen Li, Varun Jampani, Yael Pritch, Michael Rubinstein, and Kfir Aberman. Dreambooth: Fine tuning text-to-image diffusion models for subject-driven generation. In *Proceedings of the IEEE/CVF conference on computer vision and pattern recognition*, pp. 22500–22510, 2023.
- Nataniel Ruiz, Yuanzhen Li, Varun Jampani, Wei Wei, Tingbo Hou, Yael Pritch, Neal Wadhwa, Michael Rubinstein, and Kfir Aberman. Hyperdreambooth: Hypernetworks for fast personalization of text-to-image models. In *Proceedings of the IEEE/CVF Conference on Computer Vision and Pattern Recognition*, pp. 6527–6536, 2024.
- Jing Shi, Wei Xiong, Zhe Lin, and Hyun Joon Jung. Instantbooth: Personalized text-to-image generation without test-time finetuning. In *Proceedings of the IEEE/CVF Conference on Computer Vision and Pattern Recognition*, pp. 8543–8552, 2024.
- Aleksandar Shtedritski, Christian Rupprecht, and Andrea Vedaldi. What does clip know about a red circle? visual prompt engineering for vlms. In *Proceedings of the IEEE/CVF International Conference on Computer Vision*, pp. 11987–11997, 2023.
- David Wan, Jaemin Cho, Elias Stengel-Eskin, and Mohit Bansal. Contrastive region guidance: Improving grounding in vision-language models without training. In *ECCV*, 2024.
- Peng Wang, Shuai Bai, Sinan Tan, Shijie Wang, Zhihao Fan, Jinze Bai, Keqin Chen, Xuejing Liu, Jialin Wang, Wenbin Ge, et al. Qwen2-vl: Enhancing vision-language model’s perception of the world at any resolution. *arXiv preprint arXiv:2409.12191*, 2024.
- Jianwei Yang, Hao Zhang, Feng Li, Xueyan Zou, Chunyuan Li, and Jianfeng Gao. Set-of-mark prompting unleashes extraordinary visual grounding in gpt-4v. *arXiv preprint arXiv:2310.11441*, 2023.
- Chun-Hsiao Yeh, Bryan Russell, Josef Sivic, Fabian Caba Heilbron, and Simon Jenni. Meta-personalizing vision-language models to find named instances in video. In *Proceedings of the IEEE/CVF Conference on Computer Vision and Pattern Recognition*, pp. 19123–19132, 2023.
- Yu Zeng, Vishal M Patel, Haochen Wang, Xun Huang, Ting-Chun Wang, Ming-Yu Liu, and Yogesh Balaji. Jedi: Joint-image diffusion models for finetuning-free personalized text-to-image generation. In *Proceedings of the IEEE/CVF Conference on Computer Vision and Pattern Recognition*, pp. 6786–6795, 2024.
- Deyao Zhu, Jun Chen, Xiaoqian Shen, Xiang Li, and Mohamed Elhoseiny. Minigpt-4: Enhancing vision-language understanding with advanced large language models. *arXiv preprint arXiv:2304.10592*, 2023.
- Xueyan Zou, Jianwei Yang, Hao Zhang, Feng Li, Linjie Li, Jianfeng Wang, Lijuan Wang, Jianfeng Gao, and Yong Jae Lee. Segment everything everywhere all at once. *Advances in Neural Information Processing Systems*, 36, 2024.

Appendices

A Ablation

In this section we ablate various aspects of our personalization method primarily using the Yo’LLaVA dataset as it serves as a well-established benchmark.

A.1 Retrieval Module Backbone

We present an ablation study of the image encoder F_{emb} , which serves as the backbone of the Retrieval Module and is responsible for extracting object features and performing matching. Table 7 shows a noticeable gap between CLIP and DINO, indicating that DINO’s visual features are more discriminative and better suited for retrieval tasks. Between the two DINO variants (base and large), the larger version delivers slightly better performance, the difference is marginal indicating that any DINOv2 backbone can be deployed.

Table 7: Feature extractor ablation. DINO features significantly outperform CLIP features.

Yo’ LLaVA Dataset				
Method/Metric	Precision	Recall		
		Positive	Negative	Weighted
DINOv2 (Large)	74.8	91	98.7	94.9
DINOv2 (Base)	75.5	90.8	98.7	94.7
CLIP (Large)	69	78.3	98.2	88.3

A.2 Number of Reference Images (N)

Since our approach does not require a training phase, a key question is how many reference images are needed for robust visual recognition of personalized objects. Figure 6 shows that our method performs well with just one reference image and matches state-of-the-art performance with two images on MyVLM dataset. On Yo’LLaVa dataset, we achieve comparable performance to Yo’LLaVa Nguyen et al. (2024) with only three images, even though the full set includes up to 10 images for some objects.

A.3 Number of Personalized Objects (P)

Another key consideration for any personalization method is its robustness to increasing number of personalized objects, particularly as more intra-category instances are introduced into the dataset. Figure 7 illustrates the performance of PeKit on the first 10 objects from the Yo’LLaVA dataset as the number of personalized objects increases incrementally from 10 to all 40 categories. While there is a slight performance drop at higher values of P , PeKit demonstrates overall stability and robustness.

A.4 Threshold Selection

In the main paper, we employ a fixed threshold of $\tau = 0.75$ across all experimental settings to determine whether a personalized object is present in an image.

Figures 8 and 9 illustrate the precision–recall trade-off for different values of τ on the Yo’LLaVA dataset. As shown, $\tau = 0.75$ achieves the highest F1-score, providing the best balance between precision and recall.

Lowering the threshold increases the number of detections but also raises the likelihood of false positives. Conversely, increasing the threshold improves precision at the cost of reduced recall, potentially causing some objects to be overlooked.

For instance, in a personalized search task such as the query “find my keys,” a high threshold may prevent the model from detecting the keys altogether, whereas a low threshold may return multiple key candidates, allowing the user to manually identify the correct one. In this study, we selected the threshold 0.75 that best

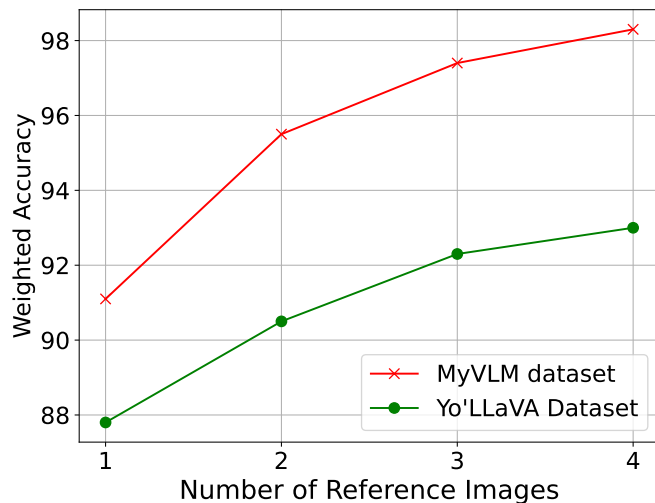


Figure 6: Ablation on N: Average weighted visual recognition accuracy as a function of number of reference images. Increasing the number of reference images improves performance, but PeKit is robust with just one reference image.

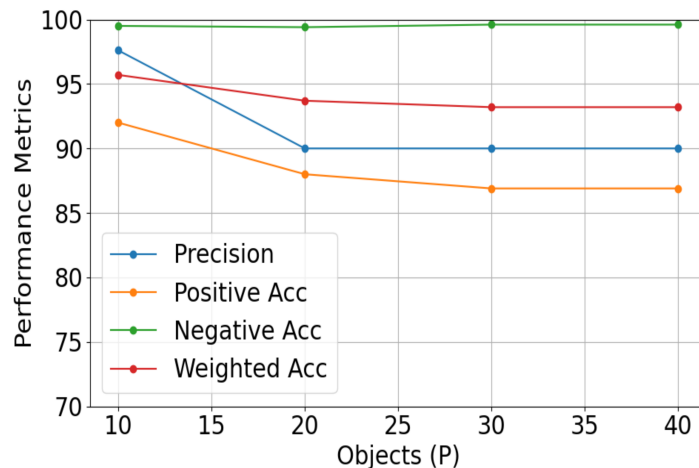


Figure 7: Ablation on P: PeKit’s performance when evaluated on a subset of 10 categories from Yo’LLaVA dataset while progressively increasing number of objects.

balances precision and recall on the Yo’LLaVA dataset and applied it across all experiments, while noting that the threshold may be adjusted depending on the requirements of a specific application.

For completeness and flexibility, we further provide a straightforward method for tuning the thresholds on a per-object basis. To adjust the threshold for a given personalized object i , we first compute the distribution of distances for the reference images of the object, and then calculate the mean μ_i and standard deviation σ_i of the distribution. The threshold is then set as $\tau_i = \mu_i - \sigma_i/2$. We note that by using this method, one can easily adjust the thresholds to be stricter or more loose by adding a scalar multiplier, as $\tau_i = \mu_i - \alpha(\sigma_i/2)$. Table 8 shows that this method can produce even higher accuracy.

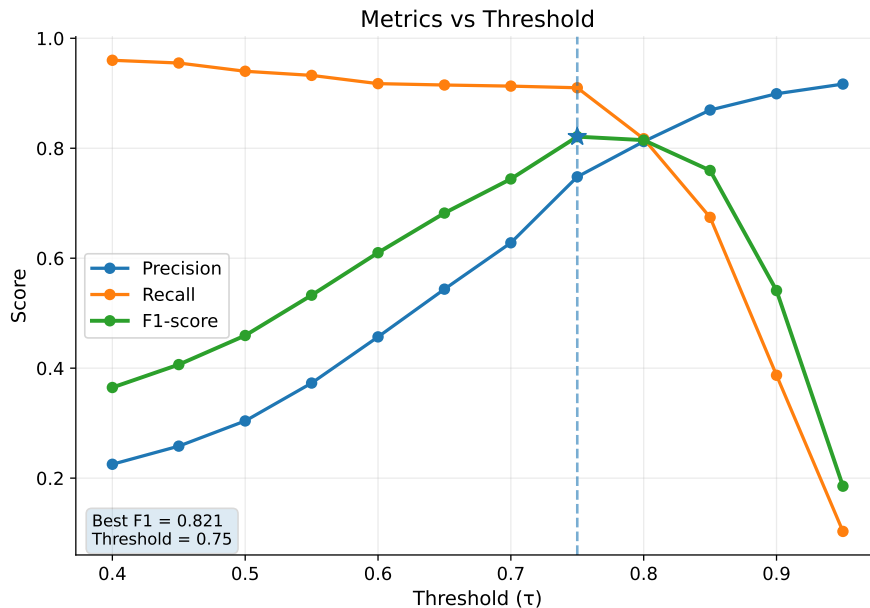


Figure 8: Precision, Recall and F1 score curve for different detection thresholds on Yo’LLaVA dataset. The best performing threshold (0.75) in terms of F1 score is marked with a star.

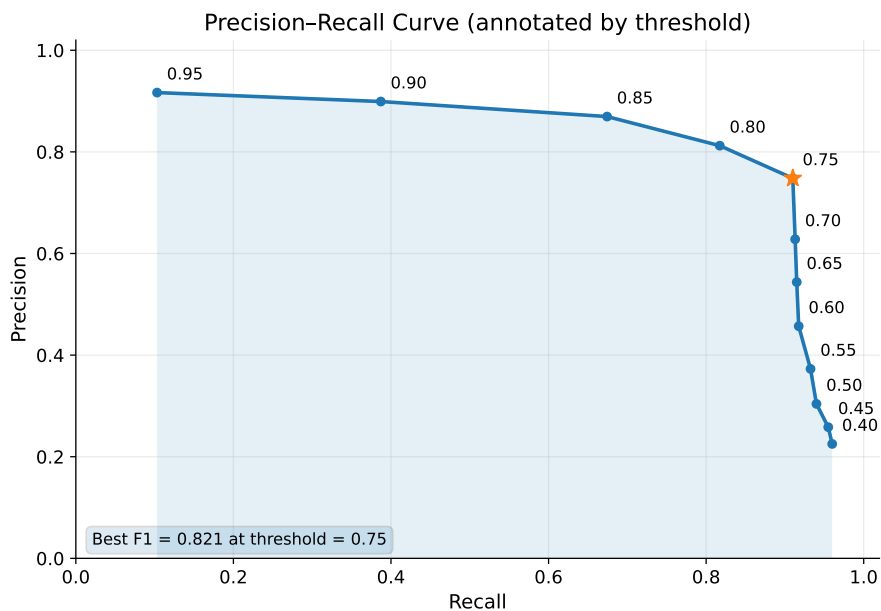


Figure 9: PR-curve on Yo’LLaVA dataset. The threshold achieving the best F1 score is marked with a star.

Table 8: Automatic object threshold selection.

Yo’ LLaVA Dataset				
Method/Metric	Precision	Recall		Weighted
		Positive	Negative	
Fixed $\tau = 0.75$	74.8	<u>91</u>	98.7	<u>94.9</u>
Tuned $\tau = \mu - \sigma/2$	<u>66</u>	92.5	<u>98.1</u>	95.3

Table 9: Video-QA naming bias ablation. Our method mitigates naming bias, improving baseline VLM accuracy in ambiguous settings without explicit object names.

Model/Variation	Base	PeKit	Base+ENTITY	PeKit +ENTITY
LLaVA-OneVision	23.0	35.0	14.0	<u>19.9</u>
InternVideoChat	56.6	61.3	45.8	<u>56.2</u>

A.5 Video-QA Object Naming

Object names often offer important contextual clues about the subject in a query to the base LVLm. For example, when asked ‘What is Jack doing?’, the model may infer that ‘Jack’ refers to a male individual in the image. In such cases, the LVLm can often respond accurately without the need for personalization. To isolate the effect of personalization, we perform an ablation study on an open-ended video QA task, where all identified personalized objects are visually prompted using the generic label ENTITY (see Appendix C and Fig.11 for prompt templates). Table 9 compares our method’s performance when using object names or the term ENTITY to the base LVLm models.

A.6 Time and Memory Requirements

Table 10 details the memory usage and runtime of the various modules in our method for the LVLm personalization task. By default, we employ GroundingDINO (Base) Liu et al. (2023c) and SAM (Base) Kirillov et al. (2023) for extracting views from reference images and proposing objects during inference, DINOv2 (Large) features for retrieving personalized instances, and LLaVA 1.5 13B as our LVLm for generating answers. All experiments were conducted using an A5000 RTX GPU. As shown in the table, our plug-and-play modules are efficient, adding minimal overhead to the original LLaVA model.

Specifically, our approach introduces an overhead of 0.35 seconds per image (0.31 seconds from G-DINO) relative to LVLm’s inference time. This overhead can be substantially reduced by employing a lightweight object proposal network such as YOLO-World Cheng et al. (2024), which runs at 55 FPS compared to G-DINO’s 3 FPS. However, as reducing computational time is not the primary focus of this work, we leave further optimization in this direction for future research.

Table 10: Time and memory requirement of PeKit. View extraction is conducted only on the reference views corresponding to each personalized object category, whereas the remaining modules are executed for every image during inference.

Module	Backbone	Time/Image (S)	Memory (GB)
View Extraction	G-DINO + SAM	0.48	1.2
Object Proposal	G-DINO	0.31	0.87
Retrieval	DINOv2	0.04	1.8
Reasoning	LLaVA 1.5 13B	0.87	16.8

B This-Is-My-Img Benchmark Details

The original This-Is-My dataset Yeh et al. (2023), designed for video-level detection of personalized objects, comprises 104 training and 582 validation short video segments spanning 15 categories. However, some of the segments are no longer available for download. Consequently, one personalized object category, ‘Alex’s Piano’ has been removed from our proposed benchmark due to the unavailability of its training segments.

B.1 Single-concept Set

Table 11 presents further details about the personalized objects and the number of frames included in the single-concept validation splits of our benchmark. We sampled every 10th frame of each validation video segment and manually assigned frames to the respective splits. Note that three categories lack a **Negative**

(Hard) set because the corresponding objects are present in every frame of their validation segments. The number of **Positive**, **Negative (Hard)**, and **Negative (Other)** frames varies between categories due to differences in segment length and the number of segments per object. In contrast, the **Fake** set was standardized, with 10 validation frames generated for each class. Figure 10 offers additional visual examples from our benchmark.

The single-concept validation also includes a VQA set comprising 70 images (5 per category). Challenging frames were manually selected, and initial question–answer pairs were generated using the GPT-4O model. These pairs were then manually refined to create a high-quality evaluation set. In line with the Yo’LLaVA framework, answers for this set are presented in an A/B multiple-choice format.

Table 11: Single-concept categories and number of frames of This-Is-My-Img benchmark. The validation frames in the dataset are organized into three subsets for each category: frames where the object is visible (*Positive*), frames from the same video segments where the object is absent (*Hard*), and positive frames belonging to other object categories (*Other*). In addition, the benchmark provides a GPT-generated set of 10 images per category (*Fake*).

Category	Positive	Negative (Hard)	Negative (Other)
Alex’s Bag	161	43	2096
Alex’s Hat	120	0	2137
Blippi’s Shoes	339	79	1918
Casey’s Boosted Board	35	118	2222
Casey’s Friend Marlan	24	4	2233
Casey’s Son	46	15	2211
Gab’s Puppy Lili	56	12	2201
Nikki’s Camper Bag	229	76	2028
Nikki’s Car	651	184	1606
Reynard’s Keyboard	162	29	2095
Reynard’s Work Chair	188	59	2069
Sherry’s Road Bike	95	12	2162
Zak’s Dog Coffee	26	0	2231
Zak’s Dog Kona	125	0	2132
Sum	2257	631	29341

B.2 Multi-concept Set

Table 12 outlines the category pairs used in our multi-concept validation benchmark. This benchmark comprises 55 images, with each category pair represented by 5 manually selected positive examples sourced from the validation frames. We extended the original This-Is-My-Img dataset categories (Table 11) by incorporating new personalized categories: Alex, Blippi, Casey, Gab, Nikki, Sherry, and Zak. For each of these added categories, we selected 5 reference views from the training segments. Each image in the benchmark is accompanied by an open-ended question–answer pair, collaboratively crafted with GPT-4O. This open-ended visual question answering (VQA) format raises the task’s difficulty and reduces the likelihood that the underlying LVLM model can succeed through answer-choice elimination alone.

Table 12: Multi-concept categories on This-Is-My-Img benchmark. Each category-pair comes with 5 positive frames and 50 negative frames from other category pairs.

Category-pair	
Alex - Alex’s Bag	Nikki - Nikki’s Car
Alex - Alex’s Hat	Nikki - Nikki’s Camper Bag
Blippi - Blippi’s Shoes	Sherry - Sherry’s Road Bike
Casey - Casey’s Boosted Board	Zak - Zak’s Dog Coffee
Casey - Casey’s Son	Zak - Zak’s Dog Kona
Gab - Gab’s Puppy Lili	

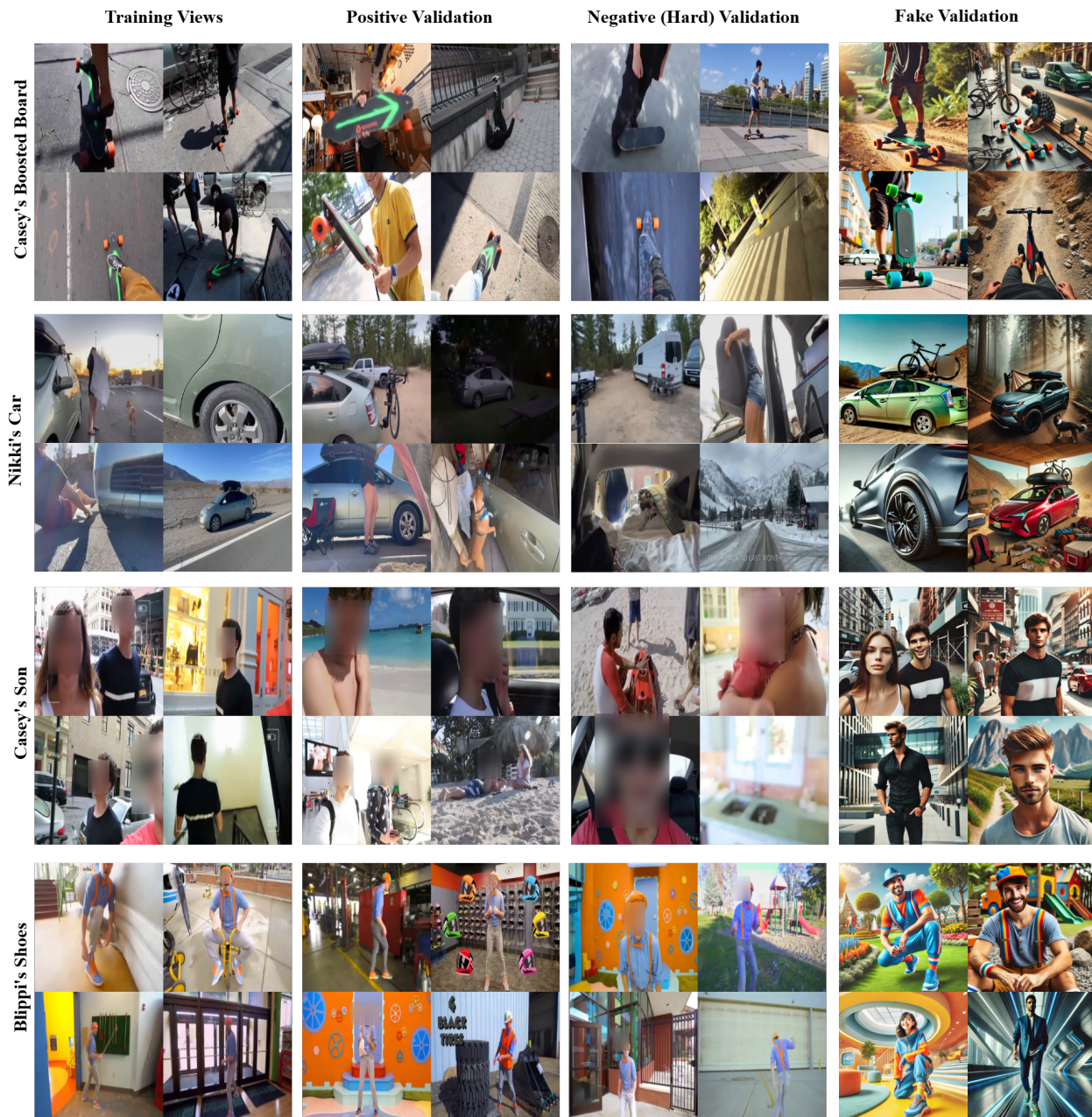


Figure 10: This-Is-My-Img single-concept benchmark. Our benchmark includes a wide range of concepts presented in realistic indoor and outdoor environments. Reference views can occasionally be sub-optimal, which increases the difficulty of the task. The positive validation set may contain false positives from within the same semantic category, allowing us to assess a model’s robustness to contextual similarities. The negative (hard) and Negative (fake) validation sets are crafted to challenge model resilience by imitating the appearance of personalized objects or their surrounding context. Additionally, the negative (‘other’) set—though not shown in this image—includes images of all other personalized objects for each concept, serving to evaluate the method’s robustness to dataset bias.

B.3 Video-QA Set

As shown in the main paper, PeKit can be extended to video personalization by applying the method to sampled frames. To evaluate this, we used validation video segments (typically under 15 seconds) and curated a VQA dataset with 267 high-quality question–answer pairs for the single-concept categories in Table 11. For each video segment, we employed the LLaVA-OneVision-Qwen2-7B model with a 1-in-16 frame sampling rate to generate an initial set of 1,380 question–answer candidates. These were then filtered for duplicates using GPT-3.5 Turbo, reducing the set to 618 pairs. Finally, we manually refined the results to produce a curated set of 267 high-quality QA pairs.

C Prompt Templates

In this section, we present the specific query format used across different parts of our experiments.

C.1 Visual prompting

As mentioned in the main paper (Sec 3.4), we employ visual prompting to indicate the personalized object’s location in the image. Next we query our LVM to personalize its answer given the instance’s name and context. Our prompt to the LVM for various tasks follows this general structure:

In this image (video), the entity enclosed in a ‘**COLOR**’ box is called ‘**NAME**’.

Without mentioning the bounding box and its color, ‘**TASK**’.

[Optional] Give more details using the information from ‘**CONTEXT**’.

The **COLOR** placeholder indicates the color of the bounding box overlaid on the image, the **NAME** placeholder specifies the instance name, and the **TASK** placeholder contains the task-specific query. Optionally, the **CONTEXT** placeholder can contain the prior knowledge about the personalized object retrieved from the memory module.

Note that when multiple objects are detected in one image, the query’s grammatical structure changes to a plural format, and the **COLOR** and **NAME** placeholders will contain multiple values separated by commas. The **CONTEXT** placeholder for each object is included in angle brackets (<>) and contains the **NAME** for the corresponding instance.

For the experiments in the paper the **TASK** placeholder can be any of the following prompts:

Personalized Captioning: Describe what is ‘**NAME**’ doing. Describe the image too.

VQA: Answer the following question about ‘**NAME**’: ‘**QUESTION**’.

Figure 11 illustrates an example of our full prompt for each one of the tasks.

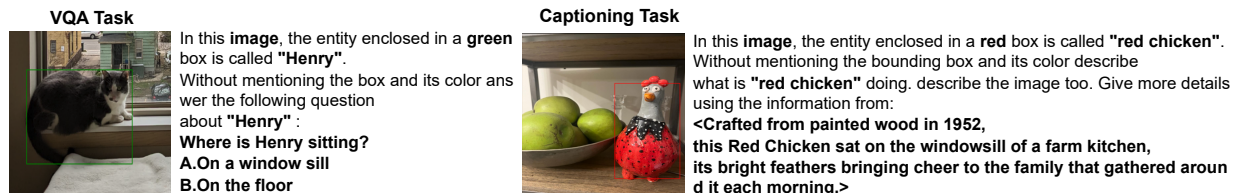


Figure 11: Prompt format. Personalized VQA and captioning on Yo’LLaVA (Left) and MyVLM (Right) datasets. The context used for the ‘red chicken’ is imaginary and generated by ChatGPT.

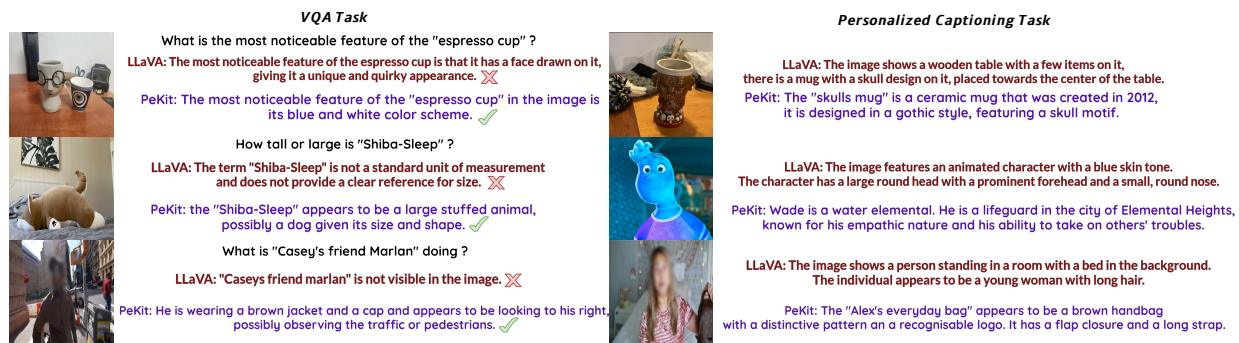


Figure 12: Qualitative comparison to LLaVA. Right: Our method detects personalized objects and integrates provided context (for qualitative comparison) in caption generation. Left: While the original model struggles with specific questions about named objects, our method easily identifies the referred object.

C.2 Open-ended VQA Validation

To evaluate the accuracy of model predictions in an open-ended VQA task, we adopt the evaluation pipeline proposed by Maaz et al. (2023). In particular, we utilize the following prompt template to query a GPT-3.5-Turbo model for assessing the semantic alignment between predicted answers and ground truth responses for each question in the VQA dataset.

‘You are an intelligent chatbot designed for evaluating the correctness of generative outputs for question-answer pairs. Your task is to compare the predicted answer with the correct answer and determine if they match meaningfully.

Here’s how you can accomplish the task: INSTRUCTIONS:

- Focus on the meaningful match between the predicted answer and the correct answer.
- Consider synonyms or paraphrases as valid matches.
- Evaluate the correctness of the prediction compared to the answer.

Please evaluate the following video-based question-answer pair:

Question: **QUESTION**

Correct Answer: **ANSWER**

Predicted Answer: **PREDICTION**

Provide your evaluation only as a yes/no answer. Please generate the response in the form of a Python dictionary string with key ‘pred’, where value of ‘pred’ is a string of ‘yes’ or ‘no’.

DO NOT PROVIDE ANY OTHER OUTPUT TEXT OR EXPLANATION. Only provide the Python dictionary string. For example, your response should look like this: ‘pred’: ‘yes’.

We calculate the VQA accuracy by dividing the number of times the GPT model, using the specified prompt template, responds with ‘yes’ by the total number of question-answer pairs in the set.

D Qualitative Results

D.1 Qualitative Comparison to LLaVA

Figure 12 presents examples of PeKit model compared to the base LLaVA Liu et al. (2023b) on VQA and personalized captioning tasks using images from all three benchmarks discussed in the main paper. When

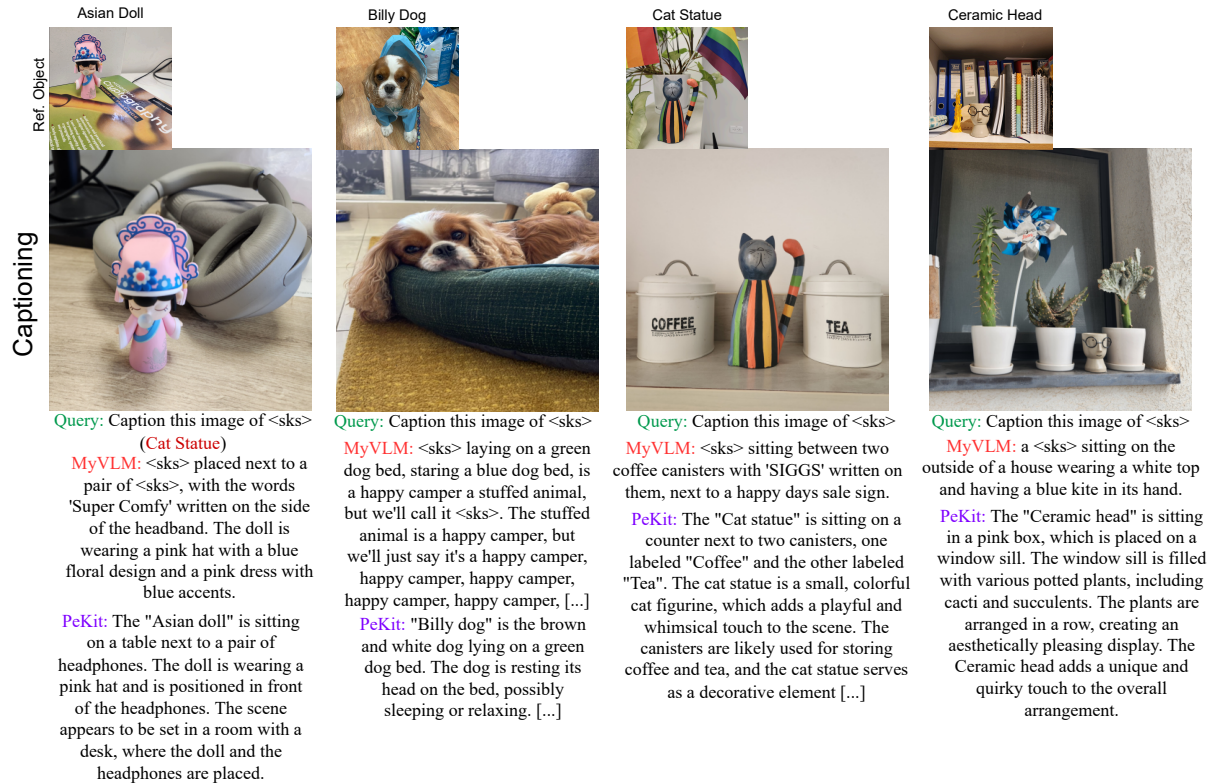


Figure 13: Qualitative comparison to MyVLM. MyVLM often misidentifies personalized objects because of its low precision. In the leftmost figure, when prompted to caption an image containing a ‘Cat Statue’—which is actually absent—MyVLM incorrectly labels the ‘Asian doll’ and the headset as the ‘Cat Statue’ instead of rejecting the query. Additionally, MyVLM training interferes with the original captioning capabilities of the LVLM, leading to hallucinations, short captions, and sometimes incomprehensible text. For each image, ‘Query’ depicts MyVLM’s system prompt where the concept identifier <sks> is replaced with the personalized object’s name. PeKit employs its own prompt template described in Appendix C.1.

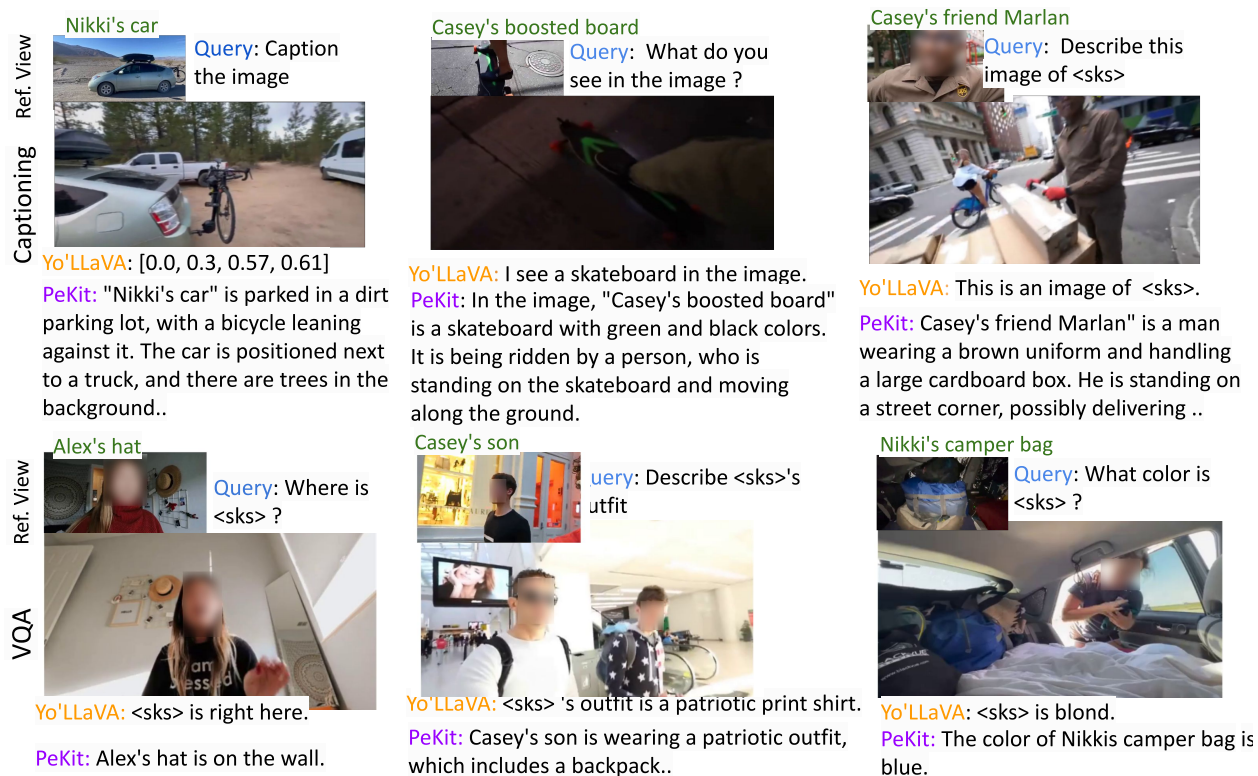


Figure 14: Qualitative comparison to Yo’LLaVA. Yo’LLaVA’s prompt template requires specifying the personalized object’s identifier in the query (first row), limiting generalization since users must already know which objects are in the image. Using image-level embeddings can also cause confusion between similar objects (e.g., Alex vs. Alex’s bag). Adjusting the LLM’s head weights further harms captioning quality. PeKit achieves better captioning quality without any training. In each example, the ‘Query’ shows Yo’LLaVA’s prompt with the concept identifier replaced by the object’s name and an added system prompt. PeKit uses a different template, detailed in the Appendix C1.

LLaVA does not recognize an object from the given name in the query, it makes guesses, leading to hallucinations or incorrect statements. In contrast, PeKit accurately identifies objects and uses in-context information to guide LLaVA in answering questions or providing details about the image, effectively incorporating in-context information and object appearance. While more advanced prompting or personalized response examples could enhance PeKit, we opted for simplicity and standard design, leaving such improvements for future work.

D.2 Qualitative Comparison to MyVLM Alaluf et al. (2024)

Figure 13 compares PeKit with MyVLM on images from the MyVLM dataset. We used the original checkpoints and code provided by the authors of MyVLM to generate the results. Checkpoints for the VQA task were not provided.

MyVLM shares the same limitation as Yo’LLaVA, functioning exclusively when the concept identifier is included in the query. Additionally, MyVLM exhibits low precision in detecting personalized objects, as shown in the main paper for the This-Is-My-Img benchmark. This can lead to misidentifying objects as personalized ones. The leftmost image in Figure 13 demonstrates this limitation. MyVLM is asked to provide a caption for the target concept ‘Cat Statue’ while the provided image includes another personalized object, ‘Asian Doll.’ As shown, MyVLM incorrectly identifies the ‘Asian Doll’ as the ‘Cat Statue’ and generates an incorrect personalized caption. Our method addresses this issue by first detecting the correct personalized object(s) and then generating a caption based on the prompt template provided in Appendix C.1.

Furthermore, MyVLM’s training appears to degrade the original LLaVA’s captioning capabilities, leading to short captions with hallucinations and sometimes incomprehensible text, leading to a low CLIPScore as demonstrated in the main paper.

D.3 Qualitative Comparison to Yo’LLaVA Nguyen et al. (2024)

Figure 14 compares PeKit to Yo’LLaVA for VQA and personalized captioning tasks on This-Is-My-Img benchmark. As seen on the first row, Yo’LLaVA’s prompt template requires the query to include the target object’s concept identifier, making it unsuitable for general captioning tasks and tailored for Visual Question Answering. Besides, since Yo’LLaVA operates on image-level embeddings of reference views, it needs clutter-free object-centered reference views of the personalized objects. As seen on the second row, performance can decline if the personalized object is not in the foreground or if there are other objects/people interacting with the personalized object in the reference views. Besides, fine-tuning the last layer of the language model reduces the LLaVA’s captioning capabilities for Yo’LLaVA.

D.4 Real-world Demonstration

To evaluate PeKit in real-world conditions, we deploy it on a mobile manipulation robot for a “search and fetch” task (Figure 15). The robot autonomously explores an unfamiliar environment to locate and grasp a specific object, in this case a carton milk box named ‘My Milk’.

The robot, equipped with a wheeled base and a single-arm manipulator, combines mobility and dexterity for effective navigation and interaction. Exploration is guided by MORE Mohammadi et al. (2025), a pipeline that uses scene graphs and large language models (LLMs) to plan actions from a 3D panoptic map generated by OpenVox Deng et al. (2025). We enhance OpenVox with occupancy mapping and integrate PeKit to refine object labels for accurate identification.

Before deployment, PeKit’s RAG memory is initialized using a small set of target object images processed through our view extraction pipeline. Refined labels and the panoptic map are shared with MORE via ROS. To grasp the object, the robot navigates to its location, captures an RGB-D image, extracts the object mask using projected panoptic data refined by SAM Kirillov et al. (2023), and estimates a grasping pose via a

rule-based method. This enables successful retrieval of specific items—e.g., a chosen milk carton from a shelf with similar packages.

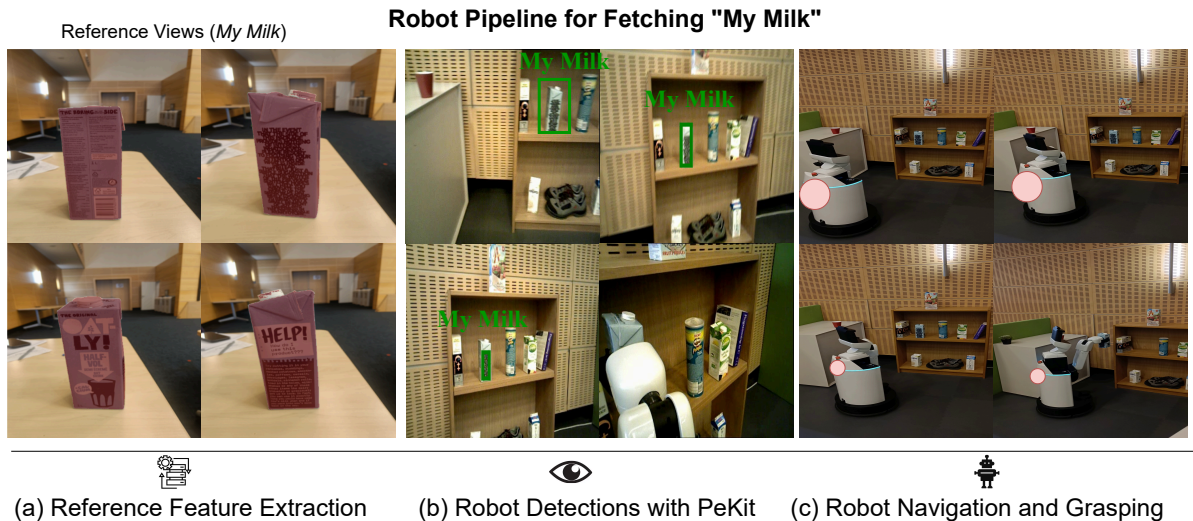


Figure 15: Real-world demonstration. PeKit can be incorporated into a mobile manipulation robot to perform personalized object search and fetching.